GEOPHYSICS, VOL. 54, NO. 11 (NOVEMBER 1989); P. 1455–1465, 12 FIGS.

Simultaneous velocity filtering of hyperbolic reflections and balancing of offset-dependent wavelets

William S. Harlan*

ABSTRACT

Hyperbolic reflections and convolutional wavelets are fundamental models for seismic data processing. Each sample of a "stacked" zero-offset section can parameterize an impulsive hyperbolic reflection in a midpoint gather. Convolutional wavelets can model source waveforms and near-surface filtering at the shot and geophone positions. An optimized inversion of the combined modeling equations for hyperbolic traveltimes and convolutional wavelets makes explicit any interdependence and nonuniqueness in these two sets of parameters.

I first estimate stacked traces that best model the recorded data and then find nonimpulsive wavelets to improve the fit with the data. These wavelets are used for a new estimate of the stacked traces, and so on. Estimated stacked traces model short average wavelets with a superposition of approximately parallel hyperbolas; estimated wavelets adjust the phases and amplitudes of inconsistent traces, including static shifts. Deconvolution of land data with estimated wavelets makes wavelets consistent over offset; remaining static shifts are midpoint-consistent. This phase balancing improves the resolution of stacked data and of velocity analyses.

If precise velocity functions are not known, then many stacked traces can be inverted simultaneously, each with a different velocity function. However, the increased number of overlain hyperbolas can more easily model the effects of inconsistent wavelets. As a compromise, I limit velocity functions to reasonable regions selected from a stacking velocity analysis—a few functions cover velocities of primary and multiple reflections. Multiple reflections are modeled separately and then subtracted from marine data.

The model can be extended to include more complicated amplitude changes in reflectivity. Migrated reflectivity functions would add an extra constraint on the continuity of reflections over midpoint. Including the effect of dip moveout in the model would make stacking and migration velocities equivalent.

INTRODUCTION

Hyperbolic reflections and convolutional wavelets are fundamental models for processing seismic data (e.g., Robinson, 1983), yet the two are rarely considered together. Deconvolution can improve the quality of common-midpoint (CMP) stacks and of semblance velocity analyses by making the recorded seismic wavelets shorter and more consistent from trace to trace. However, deconvolution does not customarily use the information gained by stacking and velocity analysis.

The normal-moveout (NMO) model assumes that the earth's impulse response is a sequence of hyperbolas in CMP gathers. Convolving traces of this impulse response with various wavelets can model isotropic sources and filtering near the surface. NMO correction of a CMP gather flattens hyperbolic reflections and makes structural information more accessible. Wavelets, on the other hand, are distorted by the NMO corrections.

Tisin (1986) estimated distorted wavelets directly by examining small time windows of NMO-corrected CMP gathers. Because the windows were short, he could model each trace with a single convolutional wavelet that had been uniformly stretched or dilated according to the amount of NMO correction.

Claerbout (1986) suggested simultaneous deconvolution of CMP gathers before and after NMO corrections to distinguish the effects of a source wavelet from those of predict-

Manuscript received by the Editor April 4, 1988; revised manuscript received May 9, 1989.
*Stanford Exploration Project, Department of Geophysics, Stanford University, Stanford, CA 94305.

able reflection coefficients (short-period multiples). He concluded that the oversimplicity of NMO corrections as a downward-continuation process limited the ability to discriminate between structural and source information.

Thomas (1986) proposed treating a deconvolved zero-offset trace as a model of reflectivity at all offsets. He modeled nonzero offset traces by stretching the zero-offset trace carefully (to preserve the magnitude of reflections). He then estimated a single convolutional wavelet that made these stretched traces best resemble the recorded traces of the CMP gather. He used this wavelet to deconvolve the zero-offset trace, restretch, and reestimate the wavelet until convergence was reached.

The above approaches use the NMO model to improve deconvolution. The opposite goal, using the convolutional model to improve stacking, remains. How do we use more than one trace to estimate reflectivity? Can we consider more than one wavelet per CMP gather? Can we consider more than one velocity function?

Static shifts are usually treated independently because they are a simple special case of the convolutional model. (A static shift is a convolution with a shifted delta function.) Ronen and Claerbout (1985) and Rothman (1986) have shown how to determine static corrections based on the quality of the hyperbolic stack at chosen velocities. Determining statics and (residual) velocities simultaneously is difficult unless structure is assumed to be flat (Schultz, 1985).

Hutchinson and Link (1984) and Thorson and Claerbout (1985) separated multiple and primary reflections by modeling them as superpositions of hyperbolas with different velocities; the unwanted multiples could be modeled separately and subtracted. If this model-based estimate of reflectivity could incorporate the undistorted convolutional wavelets of Thomas (1986), it should be possible to model reflections with greater accuracy than by either method alone.

This paper does not aim to go beyond the assumptions of the hyperbolic and convolutional models but rather to find the simplest means of considering the two together. Instead of defining the stacked section and convolutional wavelets by means of an algorithm, I shall treat them as parameters in equations that model the data. To invert these equations, a damped least-squares objective function is optimized iteratively by a conjugate-gradient algorithm. An optimized inversion of the equations must consider the overlapping effects of the parameters on the data. Accurate estimation of stacking velocities is made unnecessary by including a number of stacks with different stacking-velocity functions.

ASSUMPTIONS OF THE NORMAL MOVEOUT AND CONVOLUTIONAL MODELS

A hyperbolic NMO equation makes very restrictive physical assumptions, but it can be extended for more complicated reflections. CMP gathers include all shot positions s and geophone positions g with identical midpoint coordinates $y = (s + g)/2$. Each gather is arranged by the offset coordinate $h = (g - s)$. If an impulse expands through a medium of constant velocity v and reflects from a flat interface, the traveltime t is given by

$$t^2 = t_0^2 + \frac{h^2}{v^2}, \tag{1}$$

where t_0 is the traveltime at zero offset.

For a dipping layer, the equation remains exact if v is set equal to the medium velocity divided by the cosine of the layer's dip (Levin, 1971). Alternatively, reflection times from a horizontally stratified medium (layers are flat; velocity changes only vertically) can be approximated to second order in h if v is replaced by the root-mean-square (rms) velocity:

$$[v_{\text{rms}}(z)]^2 = \frac{\int_0^z v(z')\, dz'}{\int_0^z [v(z')]^{-1}\, dz'}, \tag{2}$$

where z is the vertical depth. With dip correction, rms velocity can be extended to nonflat layers. A linear superposition of hyperbolic reflections can also model refections from curved and diffracting interfaces.

The NMO model assumes that the data represent an impulse response; that is, the shots and geophones have impulsive radiation patterns. Surface-consistent convolution assumes that the earth's impulse response has been filtered independently at the shot and geophone positions to create the recorded data. Because convolution is time-invariant, it cannot easily model filtering at greater depths—a problem for tomographic inversion. Similarly, convolution cannot easily model angular changes in reflection coefficients if more than one reflection appears in the data.

Let $w_s(s, t)$ model the shot waveform as filtered at the near surface, and let $w_g(g, t)$ model filtering near and by the geophone. The data can be modeled by

$$\text{data}\,(y, h, t) = \text{impulse}\,(y, h, t) * w(y, h, t),$$

where

$$w(y, h, t) = w_s(y - h/2, t) * w_g(y + h/2, t). \tag{3}$$

The wavelets within a single midpoint gather (with a common y) share no surface-consistent wavelets. Each offset possesses an independent wavelet.

At first sight, it appears easiest to estimate the smaller number of surface-consistent wavelets on the right side of equation (3) rather than an independent wavelet for each midpoint and offset. However, note that the data are a linear function of the independent wavelets but not of the surface-consistent wavelets. As an example of the resulting complications, all shot wavelets could be given an arbitrary phase shift and geophone wavelets the negative of that phase shift without affecting $w(y, h, t)$. It would be useful to know first how much information the data provide for a direct estimate of independent wavelets (one for each trace). Then one could consider how much additional help, or hindrance, surface consistency would provide.

The usual goals of these models are (prestack) deconvolution and NMO stack. To see the implicit constraints on the data, one could try to reverse the normal processing sequence to reconstruct the data from the stacked traces and convolutional wavelets.

Imagine that a stacked seismic profile represents, as post-stack migration assumes, a zero-offset impulse response. Each stacked trace can be reverse corrected according to its NMO velocity function to model an entire midpoint gather. The stack does not preserve information on changes in amplitude and phase with offset, so the reverse NMO correction must make simple assumptions on the geometric spreading of reflections, frequency absorption, and changes in reflection coefficients with angle. If several stacked sections are available, then one can sum their modeled gathers to create reflections, such as primaries and multiples, that arrive simultaneously with different velocities. Finally, each trace can be convolved with corresponding wavelets. This sequence of steps is defined next with simple modeling equations.

A MODEL FOR MIDPOINT GATHERS

Let us begin with a model for a single midpoint gather. Choose a set, indexed by j, of rms velocity functions $v_j(t_0)$ that cover all reasonable primary and multiple velocities. Let $r_j(t_0)$ be the corresponding "deconvolved stacked" traces that contain the amplitudes and zero-offset arrival times of reflections—call them reflectivity functions. The following equation maps each point of a reflectivity function to a hyperbola over offset:

$$\text{hyp}_1(h, t) = \sum_j \int \delta\left[t - \sqrt{t_0^2 + h^2/v_j^2(t_0)}\right] r_j(t_0)\, dt_0. \quad (4)$$

If the reflectivity function contains an impulsive delta function, then the impulsive hyperbolic reflection is constant in strength over offset. If a reflectivity function contains a band-limited pulse, the hyperbolic waveform changes in amplitude over offset but not in area.

Thomas (1986) created nonzero offset traces from a deconvolved zero-offset trace by an interpolation scheme that also preserved the reflectivity strength over offset. Equation (4) would apply an identical stretch to a single reflectivity function if the delta function were replaced by a square gate with a width equal to the sampling rate.

When used directly in discrete form, equation (4) is convolved with a tapered sin $(t)/t$ function (a sinc function) that is band-limited to the Nyquist frequency of the data (Bracewell, 1978). The convolution replaces the delta function by the sinc function.

To integrate equation (4) analytically, note that the delta function is equivalent to a sum of delta functions positioned at the zeros of the argument and divided by derivatives of the argument (Bracewell, 1978). If the velocity function has a significant derivative, the integration must sum over multiple zeros with clumsy scale factors. For constant-velocity functions,

$$\text{hyp}_1(h, t) \cong \sum_j r_j\left(\sqrt{t^2 - h^2/v_j^2}\right) \frac{t}{\sqrt{t^2 - h^2/v_j^2}}. \quad (5)$$

This form is identical to that used by Thorson and Claerbout (1985) but with a scaling of amplitudes over offset. For velocity-space filtering, this form is best; but it becomes very inconvenient when convolved with wavelet in time.

To model one CMP gather, convolve each trace of the hyperbolic reflections in equation (4) with a wavelet. The integration over time removes the delta function:

$$\widehat{\text{data}}_1(h, t) = w(h, t) * \text{hyp}_1(h, t) = \sum_j \int w\left[h, t - \sqrt{t_0^2 + h^2/v_j^2(t_0)}\right] r_j(t_0)\, dt_0. \quad (6)$$

As a simple example, the reflectivity functions in Figure 1a are first mapped to the hyperbolas of Figure 2a with equation (4). The two nonzero reflectivity functions correspond to constant velocities of 1.4 and 2 km/s (labeled in squared reciprocal velocity, or squared slowness). Only three nonzero samples (reflections) appear—two with the same velocity and two with the same zero-offset traveltime. Note that the length and amplitude of the sinc wavelet are constant with offset in Figure 2a, unlike an NMO-stretched wavelet.

Figure 1b contains a set of convolutional wavelets; three are inconsistent in phase. Figure 2b shows the convolution of these wavelets with the corresponding traces of Figure 2a. Many high frequencies are lost, and the zero-offset traveltimes of the reflections are more ambiguous.

Clearly, modeling equation (6) is not completely invertible. The transformation destroys information in the phase and amplitude spectra of the convolutional wavelets and reflectivity functions. For instance, the polarities of the reflectivity functions and wavelets could be reversed simultaneously without affecting the modeled data. Frequencies missing from wavelets cannot be recovered in the reflectivity without using statistical constraints.

Numerically, nonuniqueness can be worse still. The less that NMO stretches a trace and the shorter a convolutional wavelet, the more nearly the two operations commute (cf., Claerbout, 1986). Thus, the phase spectra of wavelets and reflectivity can be altered in ways that almost cancel each other's effects on the data. Fortunately, such distortions in spectra must equally affect wavelets at all offsets and reflectivity functions at all velocities. We can still hope to recog-

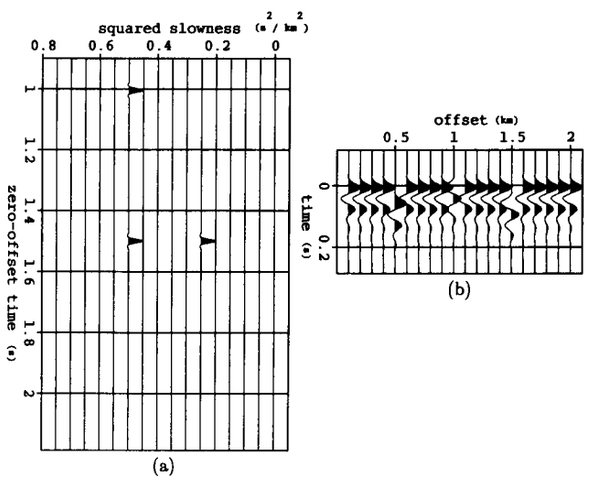

FIG. 1. (a) Two nonzero reflectivity functions with velocities of 1.4 and 2 km/s (squared slownesses of 0.5 and 0.25 s^2/km^2). (b) Convolutional wavelets, three of which are inconsistent in phase.

nize relative differences between wavelets at different offsets.

Some problems posed by one-dimensional (1-D) deconvolution can be ameliorated by inversion of the two-dimensional (2-D) model. Any single trace of Figure 2b could be regarded as having a lengthy wavelet and one reflection coefficient. One could also subdivide a wavelet and claim more than three reflections. (A statistical method of 1-D deconvolution might prefer three reflections, but more complicated wavelets and reflections make such decisions difficult.) Because different hyperbolic reflections converge with increasing offset, inversion of the 2-D model can avoid fewer than three reflections by encouraging wavelets to be as consistent as possible. Within a single reflection, the lobes of long consistent wavelets remain parallel—an easier appearance to model with convolution than with reflections at different velocities.

The NMO equation (1) describes only the initial arrival times of the wavelets, not the tails. The hyperbola that best fits the tails of wavelets corresponds to a lower velocity than a hyperbola fitting the heads of wavelets. This difference in velocity is small when wavelets are short, so a reflectivity function can still model much of the phase of consistent short wavelets.

AN OBJECTIVE FUNCTION AND OPTIMIZATION

Optimization methods improve endlessly, so I first define an inversion of relation (6) in terms of an objective function rather than by a specific algorithm. This function measures the least-squares error between the recorded and modeled data (indicated by a circumflex) and constrains the unknowns with two penalty functions (scaled by small constants a_r and a_w to ensure stability):

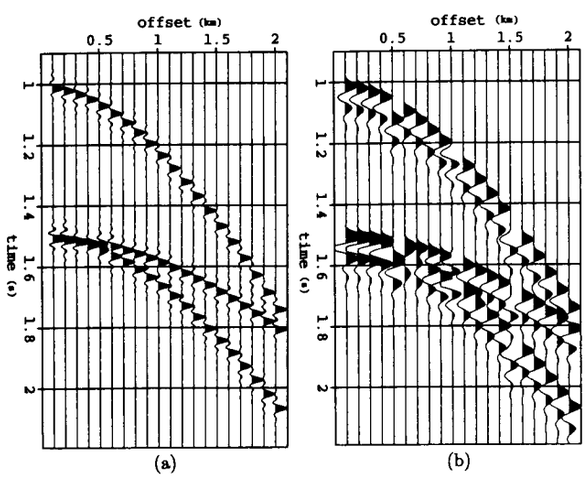

FIG. 2. (a) Three hyperbolic reflections modeled from equation (4) and the reflectivity functions in Figure 1a. Convolution with sinc functions avoids aliasing. (b) A convolution of the reflections in (a) with the wavelets in Figure 1b. High- and low-frequency information is lost, and zero-offset arrival times are more ambiguous.

$$J = \int\int \left[\text{error } (h, t)\right]^2 dh\, dt + a_r \sum_j \int \left[r_j(t_0)\right]^2 dt_0 + a_w \int\int \left[w(h, t)\right]^2 dh\, dt, \quad (7)$$

where error (h, t) = data (h, t) − $\widehat{\text{data}}_1$ (h, t).

The optimal $r_j(t_0)$ and $w(h, t)$ minimize J. The set of velocity functions $v_j(t_0)$ must be chosen beforehand. Remember that each velocity function has a corresponding reflectivity function. For convenience I write s, g, y, and h as continuous variables. Their integrals can in all cases be replaced by a sum over sampled data points.

The effect of the two penalty functions can be compared to adding a small constant to the diagonal of a possibly singular matrix before inversion (prewhitening). The penalty functions do not much affect the results of an incomplete optimization. Different optimization methods, in practice, constrain the solution differently.

Minimizing this least-squares objective function is equivalent to a maximum-likelihood estimate, assuming that noise, the reflectivity, and the wavelets are all Gaussian and white (see Kendall and Stuart, 1979). More justifiable statistical assumptions can be imagined, but this form is a convenient first choice.

Quadratic objective functions are ideal for gradient-descent methods of optimization because the required gradients are linear functions of the data. The gradient of the objective function with respect to the wavelet function (array) includes a correlation of the data error defined by equation (7) and the impulsive hyperbolas modeled by equation (4):

$$\frac{\delta J}{\delta w(h, t)} = -\int \text{hyp}_1(h, t' - t)\ \text{error } (h, t')\, dt' + a_w w(h, t). \quad (8)$$

The penalty term on the energy of the wavelet adds a term proportional to the wavelet.

The gradient with respect to the reflectivity includes an NMO stack that uses the wavelets as interpolation functions:

$$\frac{\delta J}{\delta r_j(t_0)} = -\int\int w\left[h, t - \sqrt{t_0^2 + h^2/v_j(t_0)^2}\right] \times \text{error } (h, t)\, dt\, dh + a_r r_j(t_0). \quad (9)$$

Note that J is a quadratic function of the reflectivity function or of the wavelets but not of both simultaneously. A simultaneous steepest-descent perturbation of both sets of parameters unfortunately requires an expensive line search to scale the combined gradients (8) and (9). If, however, either parameter is optimized independently, the necessary scale factor can be calculated from simple dot products (see Luenberger, 1984, on quadratic objective functions). If the wavelets are not allowed to change, then the optimum reflectivities are a linear function of the error, and vice versa.

I optimize objective function (7) alternately with respect to the wavelets and reflectivity:

(1) Assume that wavelets are impulse functions and find the optimum reflectivity functions.
(2) Leaving reflectivity functions unchanged, find the optimum wavelets. If unsatisfied, go on.
(3) Reestimate the reflectivity functions with the new wavelets, then return to step (2).

Each step solves an overdetermined least-squares problem. This procedure has little chance of optimizing the objective function completely. The first estimated wavelets will explain only what the reflectivity cannot; the next estimate of the reflectivity explains what these wavelets cannot; and so on. The procedure will not work at all if phases are too inconsistent: step (1) will be unable to model the very nonhyperbolic reflections, and step (2) will have nothing to improve upon.

The reflectivity and wavelets in Figures 3a and 3b were each reestimated three times. Only two constant-velocity functions were included in the model—those at the two correct velocities corresponding to 1.4 and 2 km/s. Each least-squares optimization used four conjugate-gradient steps. The modeled data are barely distinguishable from the original data when plotted at the same scale. The rms amplitude of the difference between the modeled and original data is less than 1 percent of the original data.

The three reflections appear in the reflectivity functions with the average phase and amplitude of the wavelets, unlike the original impulses. The estimated wavelets are approximately zero phase with time shifting, unlike the original wavelets. The reflectivity functions model a consistent average wavelet with a superposition of approximately parallel hyperbolas. As predicted, the estimated wavelets model only relative changes in phase and amplitude that cannot be modeled by the reflectivity.

These results do not have such high resolution as those obtained by Thomas (1986) from noiseless, synthetic data. When data are noiseless, one can remove all damping from the estimated parameters and minimize errors in the data down to machine precision (at the risk of numerical instability). A majority of Thomas's iterations only slightly modified the wavelet and modeled data, but they greatly improved the phase and frequency content of his reflectivity function.

The magnitude of noise in recorded data can easily exceed that of the error in these modeled data, so recorded data will have even less resolving power. If objective function (7) has a broad flat minimum, then gradient-descent methods cannot reach the vicinity of the global minimum in a small number of steps. There is not much point in continuing to descend, however, if we are only marginally improving the modeling of noise.

The preceding example demonstrates that information about the absolute phase of wavelets is lost in the data modeled by equation (5). In fact, some information is also lost about relative differences between wavelets when stacking velocities cannot be chosen with precision.

To test an extreme case, I reestimated the same reflectivity functions using a range of constant-velocity functions. These results are shown in Figure 4a. The functions were sampled evenly over squared slowness (the reciprocal of squared velocity), for which resolution is approximately the same at high and low values. Velocities ranged from 1.2 km/s to infinity. Note that much energy appears in traces with incorrect velocities—even at infinite velocity. This panel has about the same resolution over velocity as a semblance stack, so it can be used as an invertible velocity analysis, like the velocity space of Thorson and Claerbout (1985). These reflectivities can also be used as stacked traces (usually sums

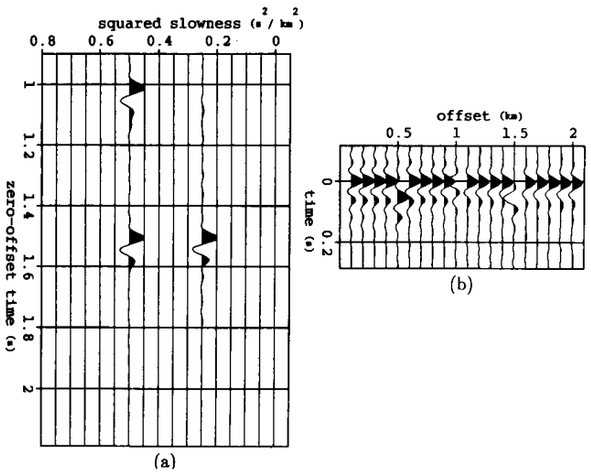

FIG. 3. (a) Estimated reflectivity functions from minimization of objective function (7). Only two correct velocity functions were included in the model; all traces with zero amplitudes were excluded. (b) Corresponding estimated convolutional wavelets. Reflectivity functions model the average phase of the reflections; estimated wavelets have approximately zero phase and differ only to adjust inconsistent traces. The modeled and original data are barely distinguishable.

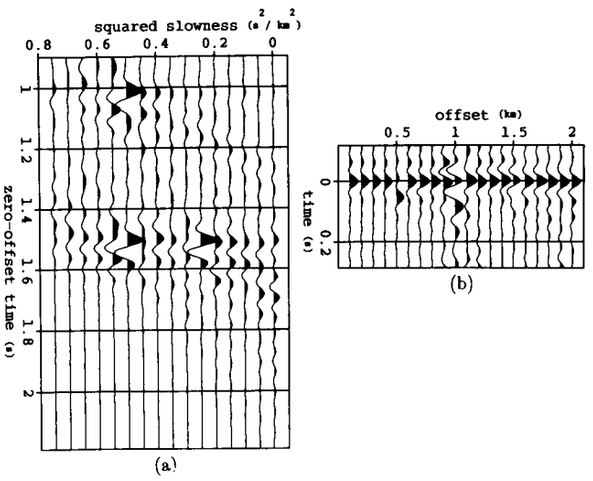

FIG. 4. (a) Estimated reflectivity functions for a large range of velocity functions. (b) Corresponding convolutional wavelets. These estimates model data as well as the results in Figure 3. Wavelets no longer accurately model inconsistent phase at large offsets because the additional overlapping hyperbolas can also model these differences.

of amplitudes over hyperbolic paths). Stacks discriminate poorly between reflections with different velocities because low offsets add coherently even when high offsets are inconsistent. Reflectivity must optimize hyperbolas at all offsets.

When combined with the convolutional wavelets in Figure 4b, these reflectivity functions model the data as well as do the more constrained results in Figure 3. The greater number of variables has increased the nonuniqueness of the modeling equation (5). The inconsistent wavelets have been estimated poorly, particularly at large offsets, because the greater number of overlapping hyperbolas can also model changes in reflections with offset.

The two extremes of these synthetic examples suggest the following rule: the more constraints placed on the velocities of reflections, the easier it is to recognize inconsistent wavelets at large offsets. (Note that surface-consistent shot and geophone wavelets affect both large and small offsets in different midpoint gathers.)

As a compromise, three velocity functions were chosen about each of the two correct velocities. Other velocities were excluded from the model. The estimated reflectivity functions in this case are shown in Figure 5a. Again large amplitudes exist at incorrect velocities, and again the modeled data are very good. This time, however, the estimated wavelets in Figure 5b are only slightly inferior to those of the well-constrained estimate in Figure 3b. A perfect knowledge of velocities would then seem to be unnecessary to estimate relative changes in convolutional filtering from trace to trace.

PHASE-BALANCING DECONVOLUTION

Assuming that the estimated wavelets express *relative* changes in phase and amplitude, one can use the wavelets to estimate what data would have resulted from a single consistent wavelet (although unknown). Such a process can be called phase balancing. To invert partially the convolution with known wavelets, minimize the following damped least-squares objective function:

$$\underset{\text{decon}(h,t)}{\text{Min}} \int\int \left[\text{data}\ (h, t) - \text{decon}\ (h, t) * w(h, t) \right]^2 dh\ dt$$

$$+ a_d \int\int \left[\text{decon}\ (h, t) \right]^2 dh\ dt. \qquad (10)$$

The gradient of this objective function with respect to the deconvolved data, decon (h, t), includes a correlation of the known wavelet with the difference between the original and modeled data. Again, four conjugate-gradient steps were used. Figure 6 shows the result of deconvolving the original data of Figure 2b with the estimated wavelets of Figure 3b.

This deconvolved gather is far from the ideal impulsive reflections of Figure 2a, but the wavelets are now consistent. A second spiking deconvolution could use the same wavelet for all traces. Consistent wavelets are also essential if one is interested in angular (not convolutional) changes in reflection coefficients.

One could model almost identical data from consistent impulsive wavelets and the reflectivity functions in Figure 3a. Deconvolution, however, preserves details that cannot be modeled in recorded data by superpositions of hyperbolas. The 1-D deconvolution is also less likely to create spurious reflections.

VELOCITY FILTERING

To demonstrate loose constraints on velocities, I use the recorded marine midpoint gather in Figure 7a (provided by the Geophysical Research Institute in Zhuoxian, China). Most of the reflections are sea-bottom primaries and multiples with velocities near that of water. The last strong

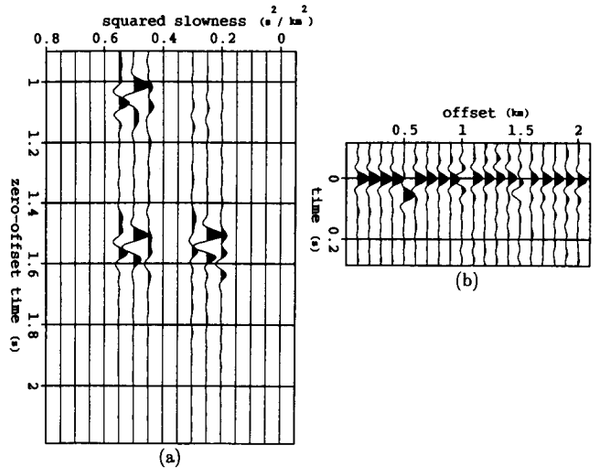

FIG. 5. (a) Estimated reflectivity functions at six velocities near the correct values. All other traces are constrained to be zero and are left out of the model. (b) Corresponding estimated convolutional wavelets. Substantial amplitudes appear in reflectivity functions at incorrect velocities, but wavelets now model changes in phase as well as did the more constrained estimates in Figure 3.

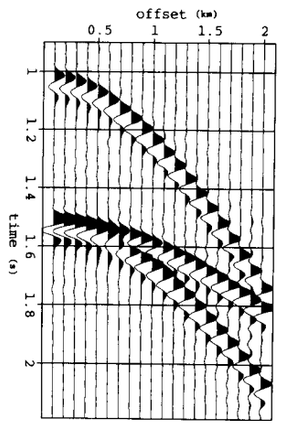

FIG. 6. A deconvolution of the data in Figure 2b with the estimated wavelets in Figure 3b. Reflections are not impulsive as in the ideal data of Figure 2a, but wavelets are now consistent.

reflection is a peg-leg multiple of the primary reflection arriving at zero offset at 1.8 s. The strength and phase of wavelets show some change with offset. Amplitudes of traces have been scaled over time to compensate for the effects of geometric spreading and the absorption of energy.

Ten velocity functions were chosen through the semblance contour plot in Figure 7b. The first five functions pass through the water-velocity reflections (the first is a primary); the second five pass through higher velocity reflections. The corresponding reflectivity functions and wavelets were estimated with the same algorithm used for the synthetic examples. The modeled data appear in Figure 8a. The difference between Figures 7a and 8a shows the uninverted reflections in Figure 8b. Higher frequencies were uninverted in the first arrivals, perhaps because the wavelets were not allowed to change their spectra with time. Other previously unseen reflections with high velocities appear in the residuals between 2 s and 2.5 s. These reflections appear as small peaks in the semblance panel of Figure 7b, but they were not included in the velocity functions.

Because the lower and higher velocity reflections are not of equal interest, I model the data again in Figure 9a with only the five lower velocity reflectivity functions. Figure 9b shows the original data minus these low-velocity reflections. The remaining data contain the high-velocity reflections, as well as all uninverted reflections. One can now view the weaker primary reflections without the distraction of water-bottom reflections.

REMOVING STATIC SHIFTS BY PHASE BALANCING

The marine-data example emphasizes the use of reflectivity information to distinguish reflections with different velocities. Convolutions were necessary only to model reflections with greater accuracy than do impulsive hyperbolas alone. Land data are less likely to have multiple reflections than do marine data; instead, filtering at the earth's weathered surface is more likely to create static time shifts such as seen in the midpoint gather of Figure 10a. (These data were recorded in the Williston Basin by Western Geophysical.) Traces shifted up or down contribute destructively to hyperbolic stacks of the data over offset. The mind's ability to imagine hyperbolic reflections makes the static shifts visible to the eye. Similarly, constraints on the hyperbolic shapes of reflections should help estimate the wavelets that describe these shifts.

First, I choose a single optimum velocity function for this gather with a modified version of Toldi's (1989) 1-D "velocity analysis without picking." Then I use four iterations of the previous algorithm to estimate a single reflectivity function and convolutional wavelets for each offset. Only the most important reflections are modeled in Figure 10b by this reflectivity. Modeled changes in reflection strengths with offset do not entirely match those of the recorded data; but the static shifts, our present goal, are modeled well. These static shifts show up clearly in the estimated wavelets in Figure 11. When the original gather is deconvolved with these wavelets (Figure 10c), the resulting reflections are

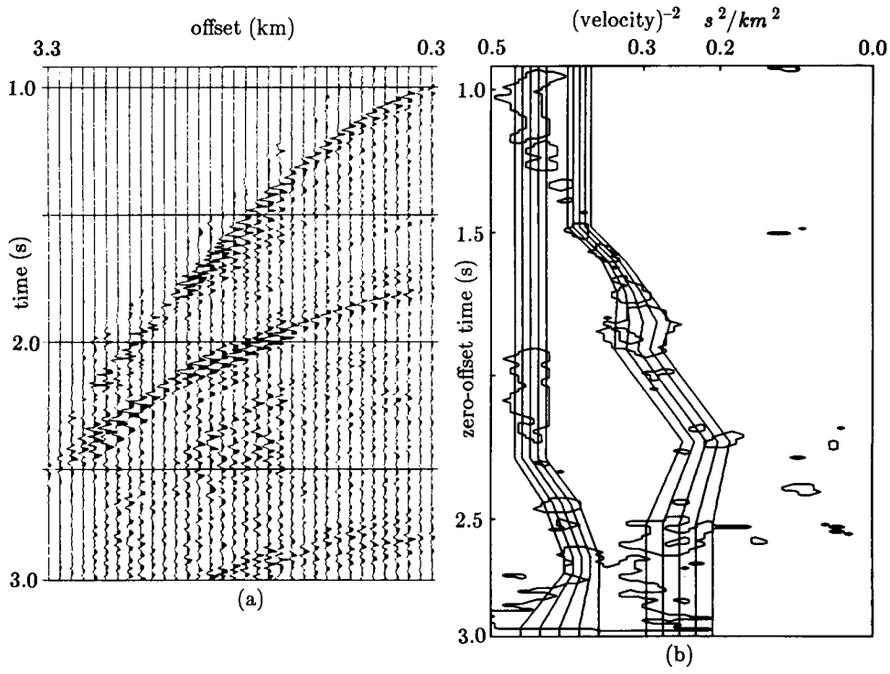

FIG. 7. (a) A marine midpoint gather provided by the Geophysical Research Institute in Zhuoxian, China. The last strong reflection is a peg-leg multiple of the primary reflection arriving at zero offset in 1.8 s. (b) A contour plot of a semblance velocity analysis of (a). Five chosen velocity functions pass through water-velocity reflections; another five pass through higher velocity primaries.

strikingly hyperbolic. A second velocity analysis finds that the reflections stack much more coherently than before.

How much of this increased hyperbolicity is reliable? The 1-D deconvolutions do not explicitly mix information across offset, so it should be difficult to create reflections that do not exist. The time-invariant deconvolutions cannot distort the curvature of one reflection without distorting the rest as well. If errors in picked velocities for different reflections cancel each other, then wavelets will not model residual hyperbolic moveout. Anyway, I use the same picked velocity functions to stack (sum) the CMP gathers over offset, so phase balancing will make these traces stack as coherently as possible.

Figure 12a shows the result of stacking 44 adjacent common-midpoint gathers. Their velocity functions are

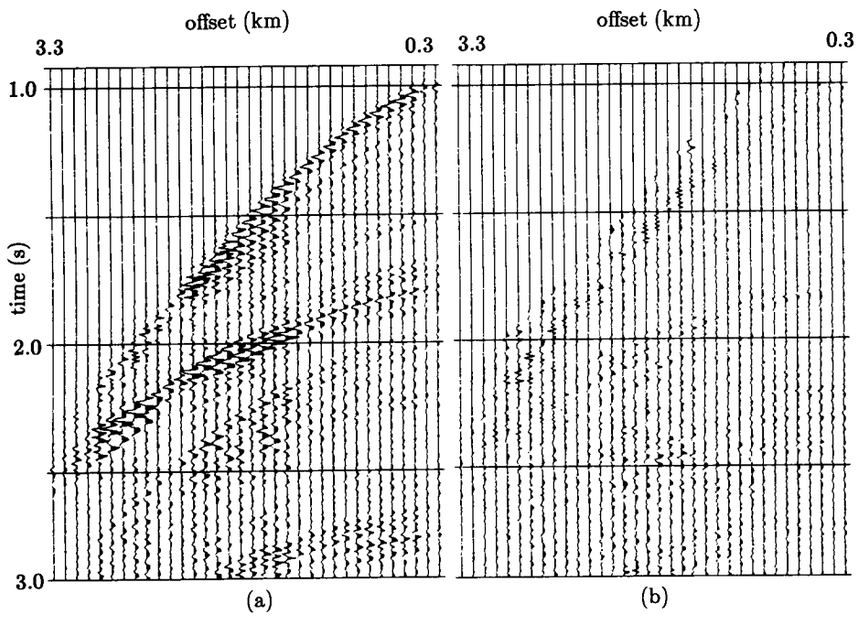

FIG. 8. (a) Reflections modeled by estimated reflectivity and convolutional wavelets. (b) The difference between the recorded data in Figure 7a and the modeled data in (a). Reflections with high velocities not included in the model appear between 2 s and 2.5 s.

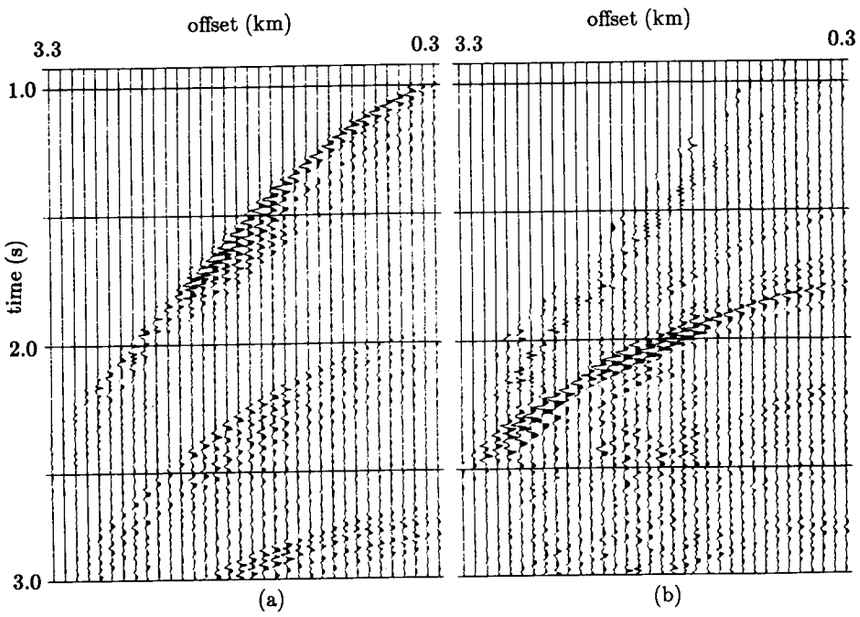

FIG. 9. (a) Reflections modeled only by the five lower velocity functions. (b) The difference between the recorded data (Figure 7a) and (a). Weaker primary reflections become more visible.

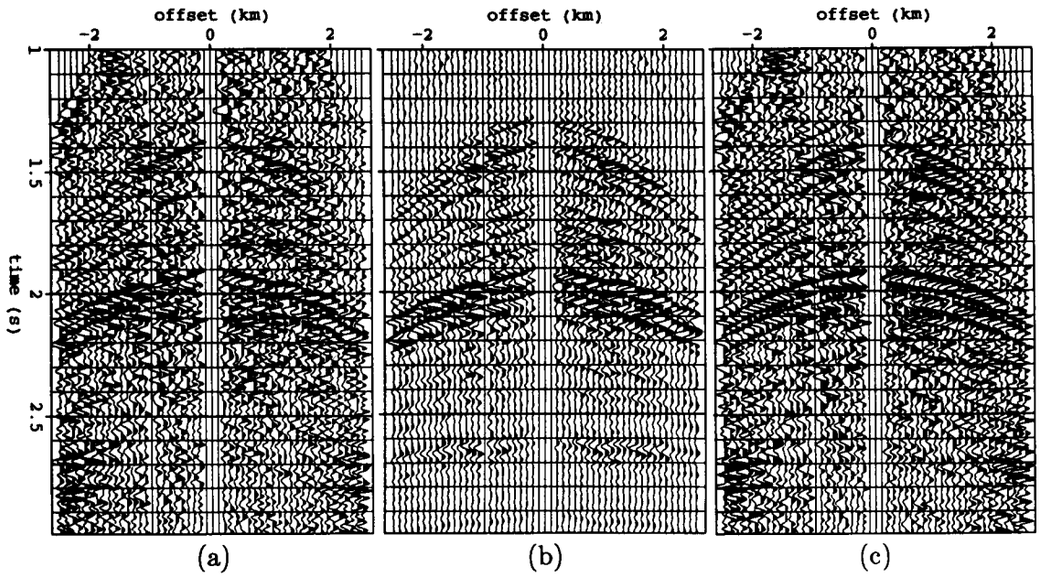

FIG. 10. (a) A land midpoint gather with strong static shifts from the Williston Basin (provided by Western Geophysical). (b) Data modeled by a single reflectivity function and the wavelets in Figure 11. (c) A deconvolution of the data in (a) with the estimated wavelets.

smoothed over midpoint to avoid abrupt changes. After stacking, traces are shifted vertically to flatten reflections and remove static shifts over midpoint (also destroying structural trends).

All gathers are phase balanced by deconvolution with individually estimated wavelets and stacked again (Figure 12b). Although deconvolved traces are renormalized to the strength of the originals, the stacked traces increase in amplitudes by about 40 percent. Reflections are cleaner because deconvolved reflections no longer sum destructively over offset. Each gather becomes internally consistent over offset, but midpoint-consistent static shifts remain; traces were shifted by the same amount as the original stack in Figure 12a.

As an alternative to stacking, the estimated reflectivity functions for each gather are shown in Figure 12c. The reflection at 2 s has increased dramatically in amplitude with respect to the other reflections. An extra double peak appears in this reflection as well. This double peak was visible in the midpoint gather in Figure 10a (the third trace in the stack), but not in either stacked section (Figures 12a and 12b). Stacking implicitly stretched and blurred the detail of this reflection. On the other hand, the reflection just before 2.5 s corresponded to an unreasonably low (multiple?) velocity that was missed by the velocity function. This reflection weakens in the estimated reflectivity because the incorrectly moved-out reflection must still fit data at all offsets.

EXTENSIONS OF THE MODEL

The previous examples ignored some common physical constraints—surface consistency, the effect of dip on moveout, and changes in amplitude with time—because they proved to have negligible effect on estimated wavelets and reflectivities. These constraints are natural first choices, however, if the model is to be generalized.

Surface-consistent convolutions of traces are independent within a single midpoint gather, but nearby midpoint gathers share many of the same shot and geophone positions [equation (3)]. A surface-consistent model needs reflectivities and velocities that are functions of midpoint:

$$\mathrm{hyp}_2\,(y, h, t) = \sum_j \int \delta\left[t - \sqrt{t_0^2 + h^2/v_j^2(y, t_0)}\right] r_j(y, t_0)\, dt_0,$$

and

$$\widehat{\mathrm{data}}_2(s, g, t) = w_s(s, t) * w_g(g, t) * \mathrm{hyp}_2\left[(s + g)/2, (g - s), t\right]. \quad (11)$$

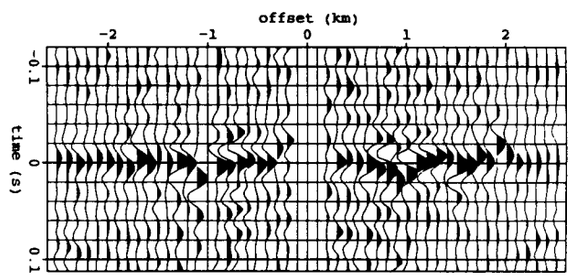

FIG. 11. Estimated convolutional wavelets for each offset of Figure 10a. Static shifts are plainly visible.

A damped least-squares objective function similar to equation (7) defines an estimate of the unknowns, but the shot and geophone wavelets cannot easily be optimized simultaneously. As before, one could alternately estimate reflectivities and shot and geophone wavelets by holding the other two sets of parameters constant.

Unfortunately, estimating the smaller set of wavelets for the land data proved just as likely to model static shifts over offset and not over midpoint. The first estimate of each reflectivity function possesses the average static shift of its midpoint gather; nearby gathers do not influence this estimate at all. Only surface-consistent wavelets, estimated later, can look at and reconcile inconsistencies between adjacent gathers. Unfortunately, these wavelets model midpoint-consistent static shifts surprisingly well. The wavelets compensate for static shifts of the reflectivity functions and discourage further improvement.

An alternative extension of our model is to add some continuity to reflections over midpoint. We do expect continuity at least over the width of the Fresnel zone, the width of the tops of diffraction hyperbolas. The reflectivity function might then be modeled by diffraction modeling of a migrated reflectivity function (e.g., Claerbout, 1985).

If the effect of dip on stacking velocities (dip moveout) is included in the model, the migration and stacking velocities should be the same (e.g., Hale, 1984). Let $\text{dipfil}_j(p, y, t_0)$ be a dip-filtered version of the reflectivity function, where $p = dt_0/dy$ (e.g., Hale and Claerbout, 1983). I define

$$\text{hyp}_3(y, h, t) = \sum_p \sum_j \int \delta\left[t - \sqrt{t_0^2 + h^2/v_j(y, t_0)^2 - h^2p^2}\right] \times \text{dipfil}_j(p, y, t_0)\, dt_0. \quad (12)$$

Other parts of the model and least-squares inversion remain unchanged.

The hyperbolic models (4) and (11) assume incorrectly that reflection amplitudes are constant with offset before surface filtering. The spreading of wavefronts and absorption of energy causes amplitudes to decrease with distance traveled. The recorded data used in this paper were scaled by the second power of time [Claerbout (1985) justifies this factor for a constant-Q material]. Local rescaling of amplitudes (automatic gain control) distorts wavelets and so should be avoided.

The previous models also assume that reflection coefficients do not change with the angle of reflection. A reflectivity function could model such changes if it were made a smooth function of the radial parameter h/vt, roughly the tangent of the angle of reflection from the vertical. A heterogeneous medium also affects amplitudes at depths between the surface and reflecting layers. Kjartansson (1979) explains how such changes depend on offset and midpoint.

CONCLUSIONS

Hyperbolic reflections and convolutional wavelets are relatively simple models for midpoint gathers, but this struc-

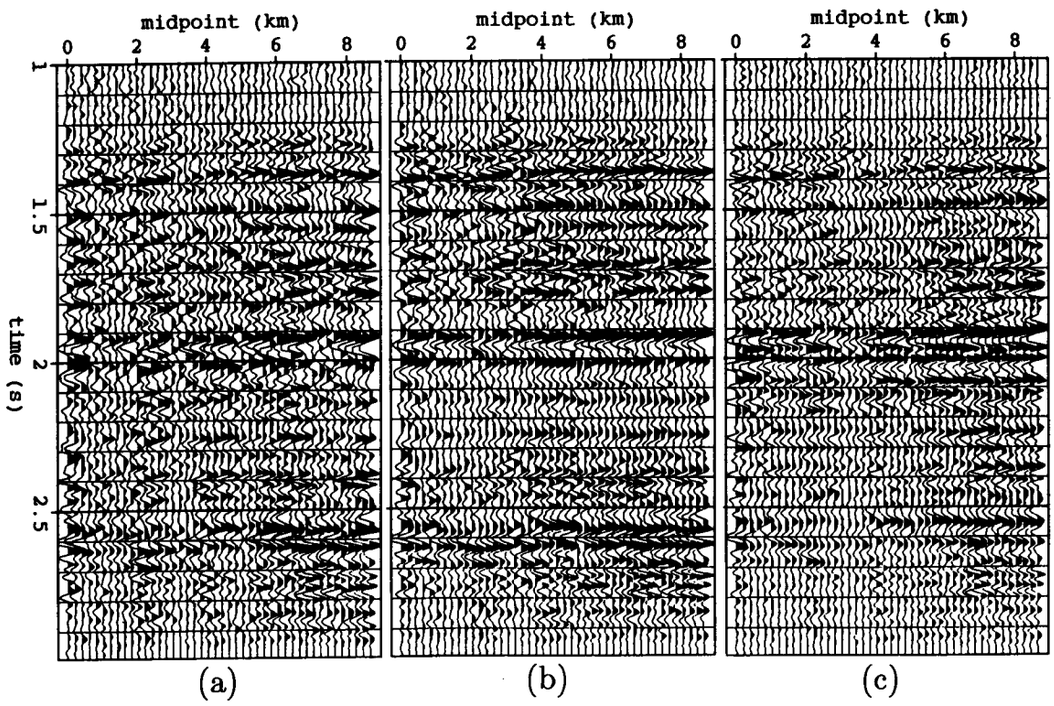

FIG. 12. (a) A stack of 44 adjacent midpoint gathers. (b) A stack of the same gathers after phase balancing. (c) The estimated reflectivity functions for the same gathers. Corresponding traces were adjusted equally after processing to remove equivalent midpoint-consistent static shifts.

ture is flexible and immediately useful. The reflectivity functions can be treated as implicitly deconvolved stacked traces, often the final result of processing midpoint gathers. The convolutional wavelets model and allow removal of inconsistent changes in phase from trace to trace—changes that are usually parameterized as static shifts. The required velocity functions are the same as those required for stacking; however, the model can include additional velocity functions to model overlapping reflections with different curvatures.

When midpoint gathers are processed independently, no assumptions need be made about changes in structure (reflectivity) from midpoint to midpoint. The convolutional wavelets have no explicit constraints except length. The convolutional form also avoids the local minima that arise when pure time shifts skip a cycle. Data need not be sampled evenly. The objective function gives equal weight to all recorded offsets and makes no assumptions about unrecorded data.

On the other hand, convolutional wavelets model only filtering of reflections near the surface, not at intermediate depths. For rms velocities to parameterize reflection traveltimes adequately, local velocities must vary slowly. The reflectivity functions as defined cannot explain any changes in reflections with offset or angle.

The optimization method allows wavelets to explain only what cannot be easily modeled by the reflectivity functions. The reflectivity can model relatively short consistent wavelets with a superposition of approximately parallel hyperbolas. The absolute phase of estimated wavelets is arbitrary—probably as close to zero phase as possible. After a phase-balancing deconvolution, statistical methods could attempt to estimate a single consistent wavelet for the entire gather.

The more exactly one constrains the velocity functions, the easier it is to distinguish the contributions of overlapping hyperbolas and inconsistent wavelets. On the other hand, a range of velocities allows one to model and suppress less desirable reflections such as multiples. The structure of the modeling equations discourages simultaneous optimization of precise velocity functions.

The least-squares inversion uses only the simplest of possible statistical constraints. One could encourage simplicity and sparseness in the estimated stacked data, as do Thorson and Claerbout (1985) or Harlan (1986). Limiting the number of modeled hyperbolas would enable wavelets to model more of the phase of short wavelets.

The number of physical parameters can be increased or decreased as suits the data or application. Gathers can be processed individually or in groups. Angular changes in amplitudes, time-adaptive wavelets, and migrated stacks can all be introduced with new parameters. This paper treats only two immediate applications of the combined hyperbolic and convolutional model. Most importantly, these examples show that the estimation of waveforms, structure, and velocities need not be pursued independently.

ACKNOWLEDGMENTS

Most of this work was completed at the Seismic Signal Processing Research Center in the automation department at Qinghua University in Beijing. The Geophysical Research Institute in Zhuoxian, China, provided the marine data with multiples. Western Geophysical provided the land data from the Williston Basin. I thank the Stanford Exploration Project for allowing me to use its facilities to complete this work.

REFERENCES

Bracewell, R. N., 1978, The Fourier transform and its applications: McGraw-Hill Book Co.
Claerbout, J. F., 1985, Imaging the earth's interior: Blackwell Scientific Publ.
——— 1986, Simultaneous pre-normal moveout and post-normal moveout deconvolution: Geophysics, **51**, 1341–1354.
Hale, I. D., 1984, Dip-moveout by Fourier transform: Geophysics, **49**, 741–757.
Hale, I. D., and Claerbout, J. F., 1983, Butterworth dip filters: Geophysics, **48**, 1033–1038.
Harlan, W. S., 1986, Signal/noise separation and seismic inversion: Ph.D. thesis, Stanford Univ.
Hutchinson, D., and Link, B., 1984, Long period multiple suppression by model fitting: 54th Ann. Internatl. Mtg., Soc. Expl. Geophys., Expanded Abstracts, 518–521.
Kendall, M., and Stuart, A., 1979, The advanced theory of statistics, v. 2, Inference and relationship, 4th ed.: Charles Griffin & Company Limited.
Kjartansson, E., 1979, Attenuation of seismic waves and applications in energy exploration: Ph.D. thesis, Stanford Univ.
Levin, F. K., 1971, Apparent velocity from dipping interface reflections: Geophysics, **36**, 510–516.
Luenberger, D. G., 1984, Linear and nonlinear programming: Addison-Wesley Publ. Co., Inc.
Robinson, E. A., 1983, Seismic velocity analysis and the convolutional model: D. Reidel Publ. Co.
Ronen, J., and Claerbout, J. F., 1985, Surface-consistent residual statics by stack-power maximization: Geophysics, **50**, 2759–2767.
Rothman, D. H., 1986, Automatic estimation of large residual statics corrections: Geophysics, **51**, 332–346.
Schultz, P. S., 1985, Seismic data processing: Current industry practice and new directions: Geophysics, **50**, 2452–2457.
Thomas, J. E., 1986, Multichannel estimate of the seismic wavelet: Geophysics, **51**, 838–843.
Thorson, J. R., and Claerbout, J. F., 1985, Velocity-stack and slant-stack stochastic inversion: Geophysics, **50**, 2727–2741.
Tisin, A. B., 1986, Design and analysis of an optimum multichannel deconvolution filter based on normal moveout stretched wavelets: Ph.D. thesis, Pittsburgh Univ.
Toldi, J. L., 1989, Velocity analysis without picking: Geophysics, **54**, 191–199.